On the role of blowing configuration for efficient drag reduction of a 3D blunt body

J.M. Camacho-Sánchez[1, 2], M. Lorite-Díez[2, 3], J.I. Jiménez-González[1, 2] and C. Martínez-Bazán[2, 3]

Grupo de Mecánica de Fluidos e Interacción Fluido-Estructura
www.mefluife-ujagr.es

---

[1] Departamento de Ingeniería Mecánica y Minera, Universidad de Jaén, SPAIN
[2] Instituto de Investigación del Sistema Tierra en Andalucía (IISTA), SPAIN
[3] Departamento de Mecánica de Estrucutras e Ingeniería Hidráulica, Universidad de Granada, SPAIN

1. Introduction

General features of heavy vehicles: Wake, drag and energy consumption

- Geometrical limitations : maximize loading capacity and simplify docking
- Wake behind heavy vehicles → fully turbulent and three-dimensional
- Low base pressure and strong recirculating zone because of a massive flow separation
- Wake contribution to drag (= fuel consumption and greenhouse gases emissions)
- Use of simplified 3D models (retains features: shedding, massive separation → high drag)

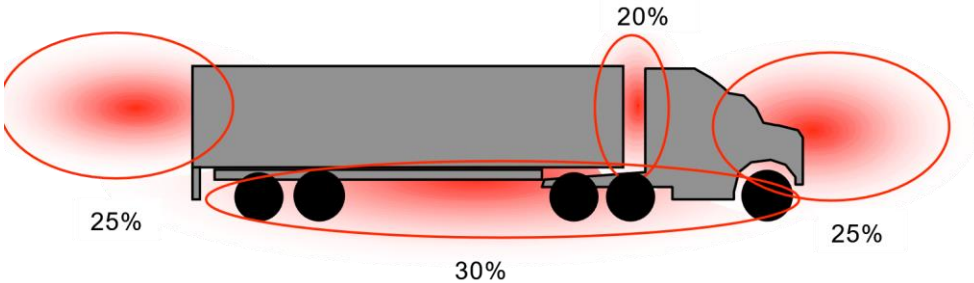

Aurell & Wadman. 2007

Square-back Ahmed body
(GM model)

Han et al. SAE 1996

1. Introduction

Blowing as a wake control technique

- Blowing is the process of injecting air
- In the present work we focus on base blowing: possibility to use exhaust gases from the engine or other sources.

➢ Perimetric base blowing in a 3D-Body

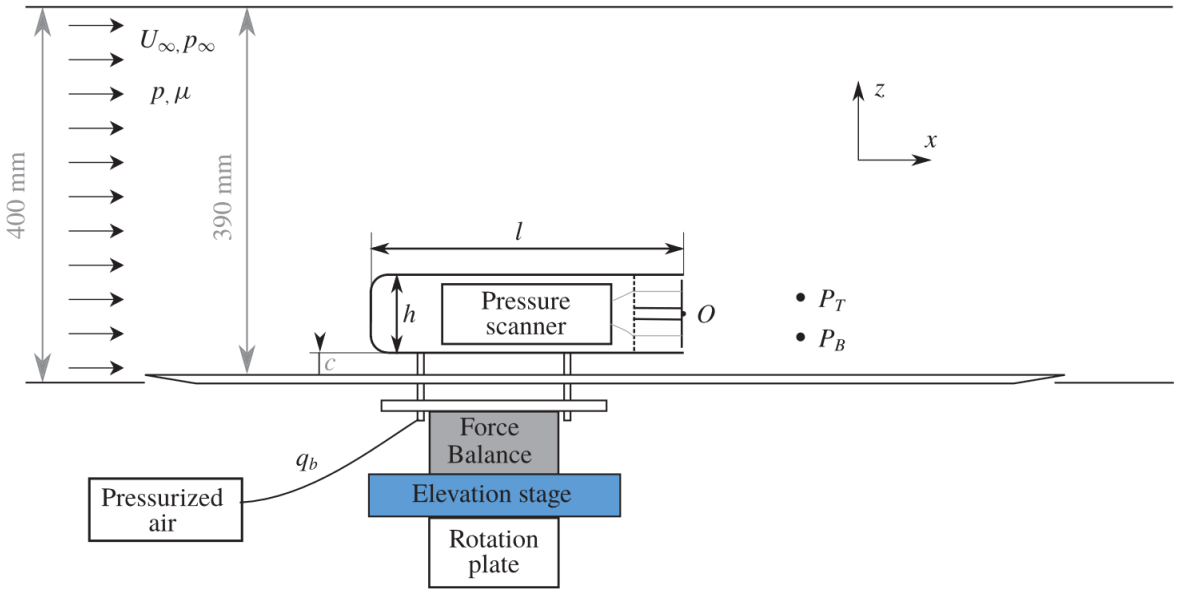

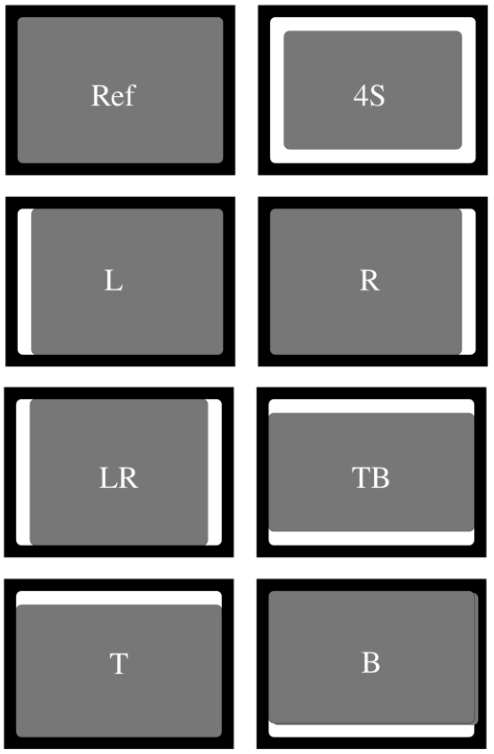

Lorite-Díez et al. JFM 2020

1. Introduction

➢ Perimetric base blowing in a 3D-Body

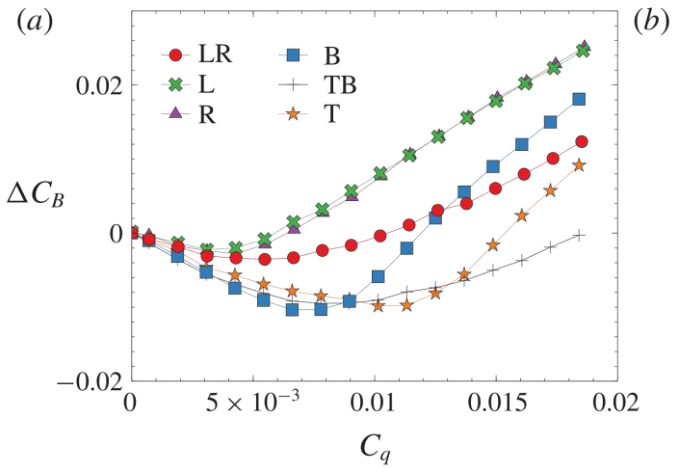

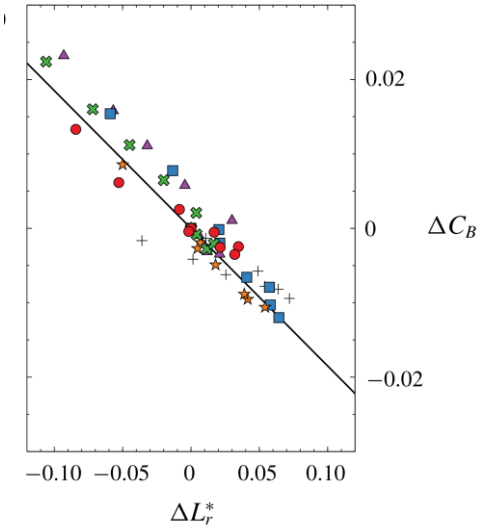

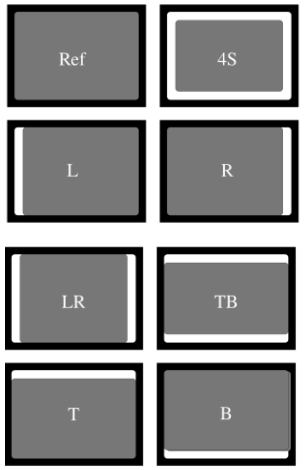

Natural

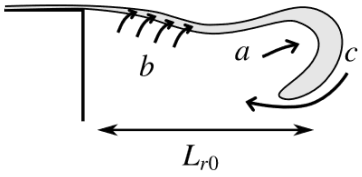

Mass regime

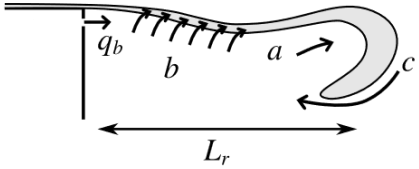

Momentum regime

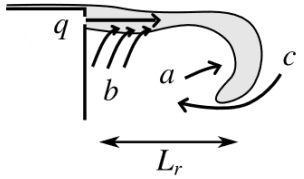

Lorite-Díez et al. JFM 2020

1. Introduction

➢ **Perimetric base blowing in a 3D-Body**

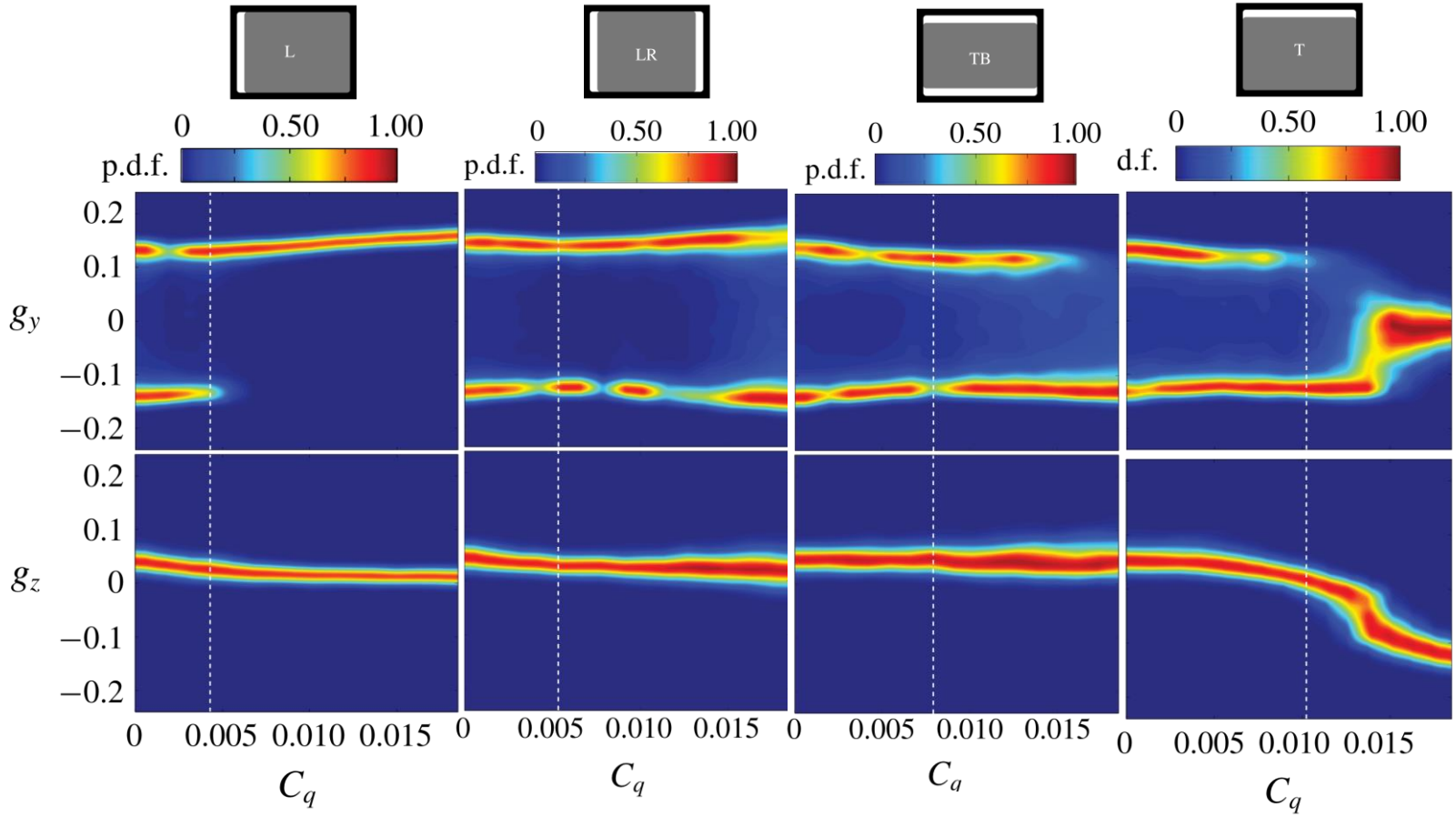

Lorite-Díez et al. JFM 2020

1. Introduction

➢ **Perimetric vs centered base blowing in a 3D-Body**

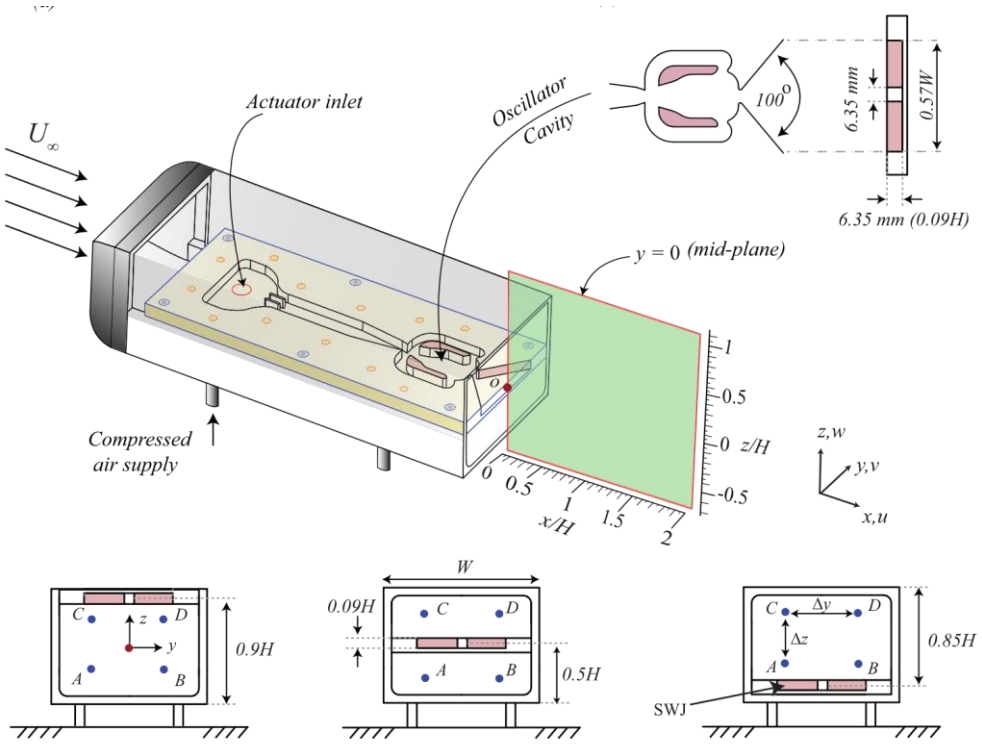

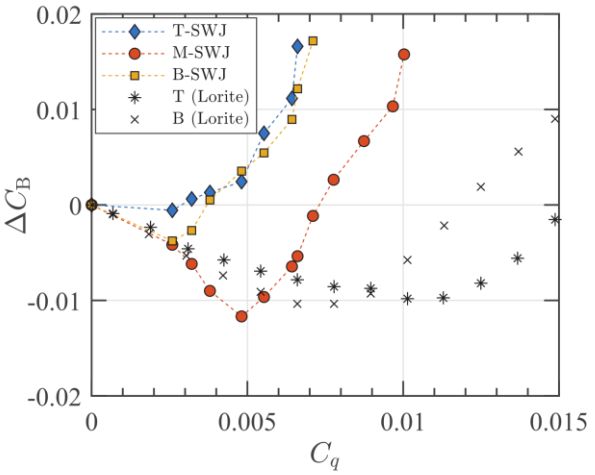

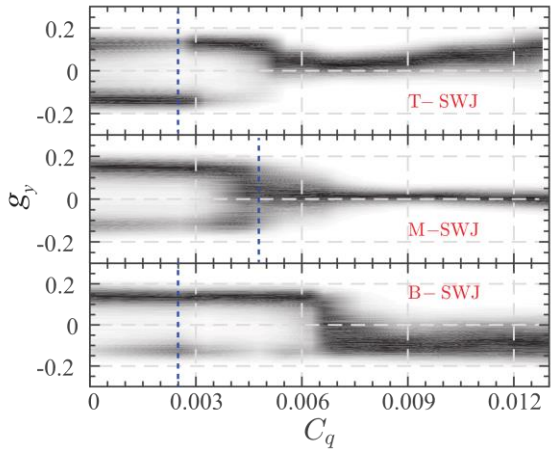

Veerasamy et al. PoF 2021

1. Introduction

➢ Centered base blowing in a 3D-Body

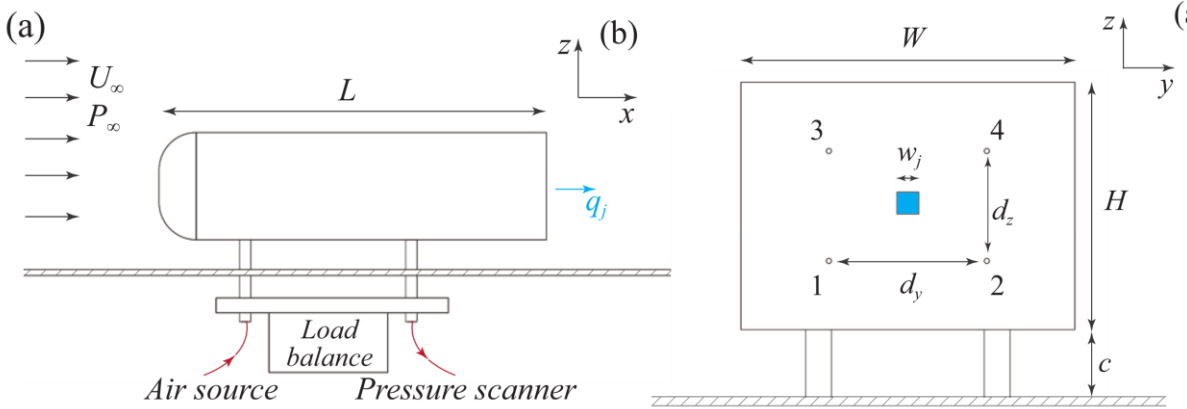

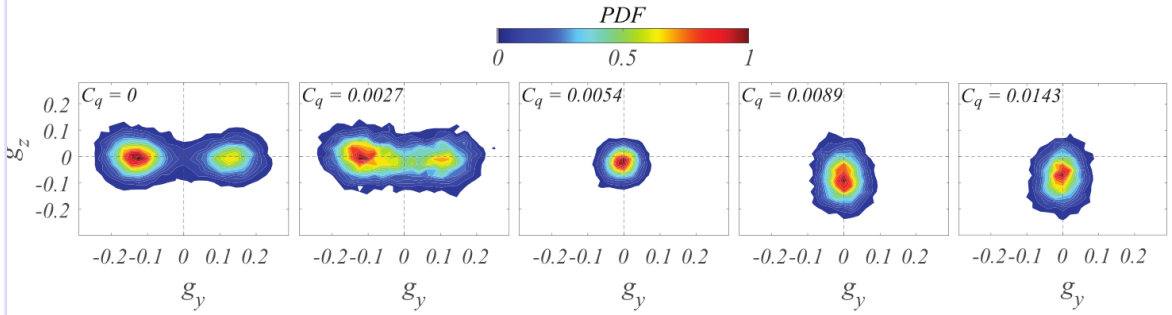

Slot	S_s/hw
x1.0	0.00570
x0.5	0.00143
x0.35	0.00070

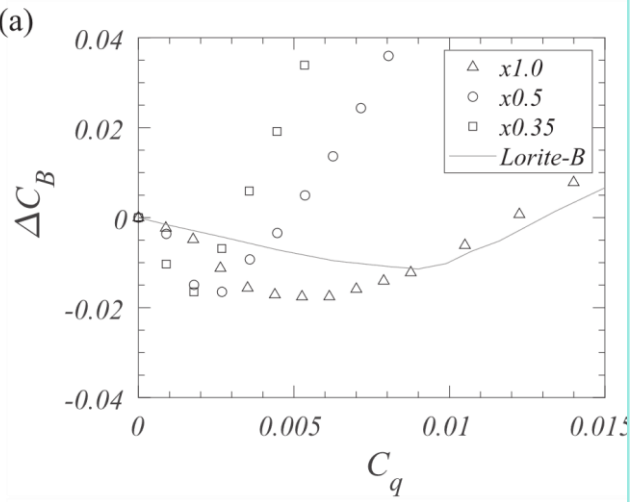

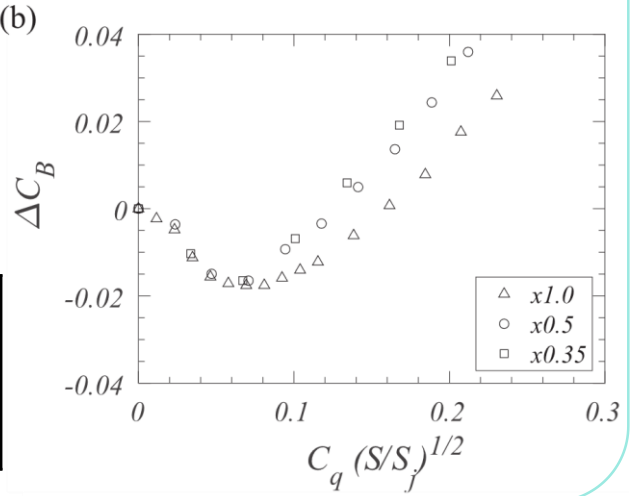

Khan et al. PRF 2022

1. Introduction

- **What is the best blowing slot configuration?**
  - Orientation: Perimetric horizontal vs Perimetric vertical (Lorite-Díez et al. 2020)

  - Location: Perimetric vs centered (Veerasamy et al. 2021)

  - Area (Khan et al. 2022)

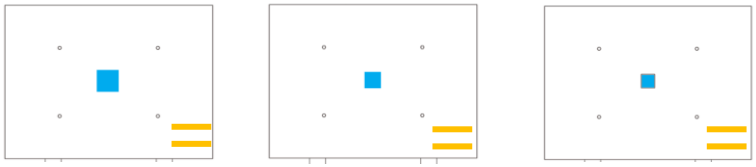

  - Shape (Present work)

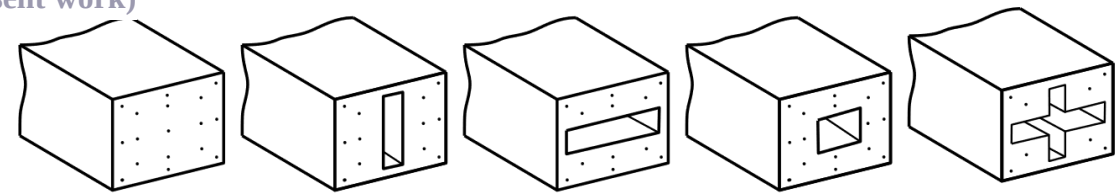

2. Experimental set-up

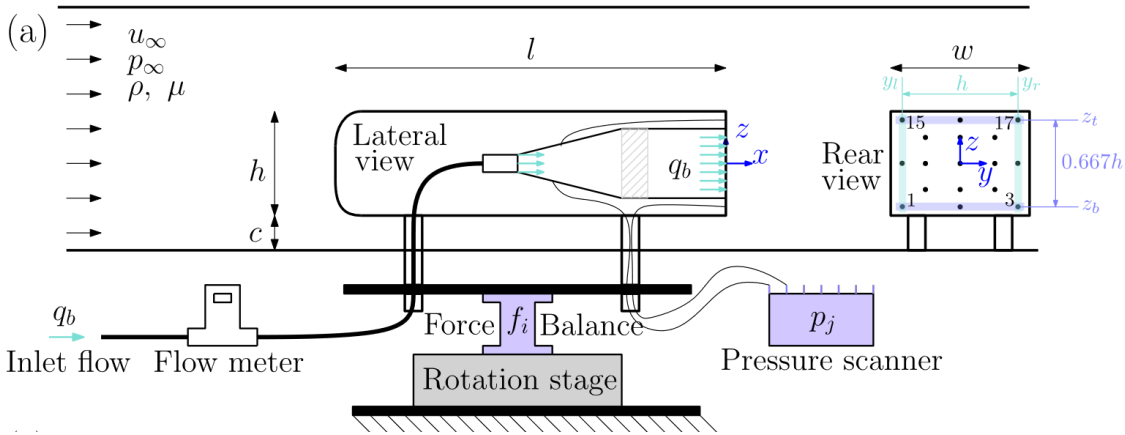

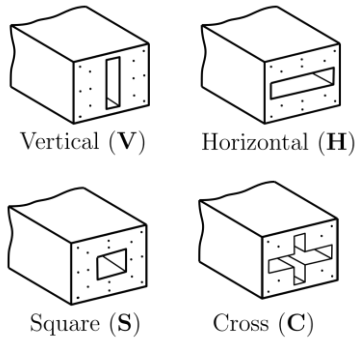

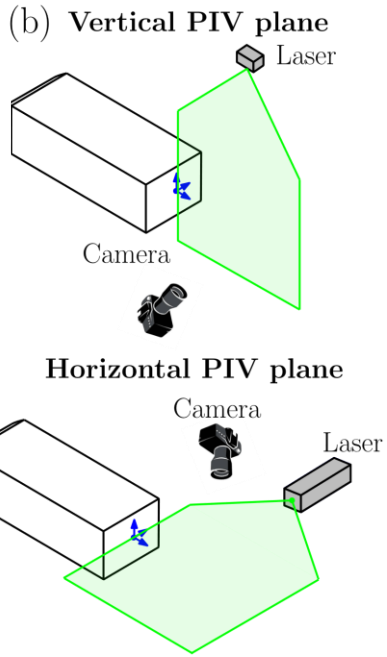

Parameters	Definition	Value
Reynolds number	$Re=\rho h u_\infty/\mu$	65000
Injected Flow rate	$c_q = (q_b s_s)/(u_\infty hw)$	[0, 0.032]
Forces coefficent	$c_i = (f_i - f_{i,b})/(0.5\rho u_\infty^2 wh)$	-
Pressure coefficient	$c_{p,j} = (p_j - p_\infty)/(0.5\rho u_\infty^2)$	-
	$c_B = -\overline{c_{p,i}}$	-
Pressure gradients	$g_y = h\frac{\partial c_p}{\partial y} \approx \frac{1}{2}\left[\frac{\sum_{j=1}^{n_{al}} c_{p,j} - \sum_{j=1}^{n_{ar}} c_{p,j}}{(y_l - y_r)/h}\right]$	-
	$g_z = h\frac{\partial c_p}{\partial z} \approx \frac{1}{2}\left[\frac{\sum_{j=1}^{n_{at}} c_{p,j} - \sum_{j=1}^{n_{ab}} c_{p,j}}{(z_t - z_b)/h}\right]$	-

Parameters	Value
h (mm)	72
w/h	1.35
l/h	3.63
c/h	0.28
$s_s/(hw)$	0.1

3. Results

➢ Wake visualizations

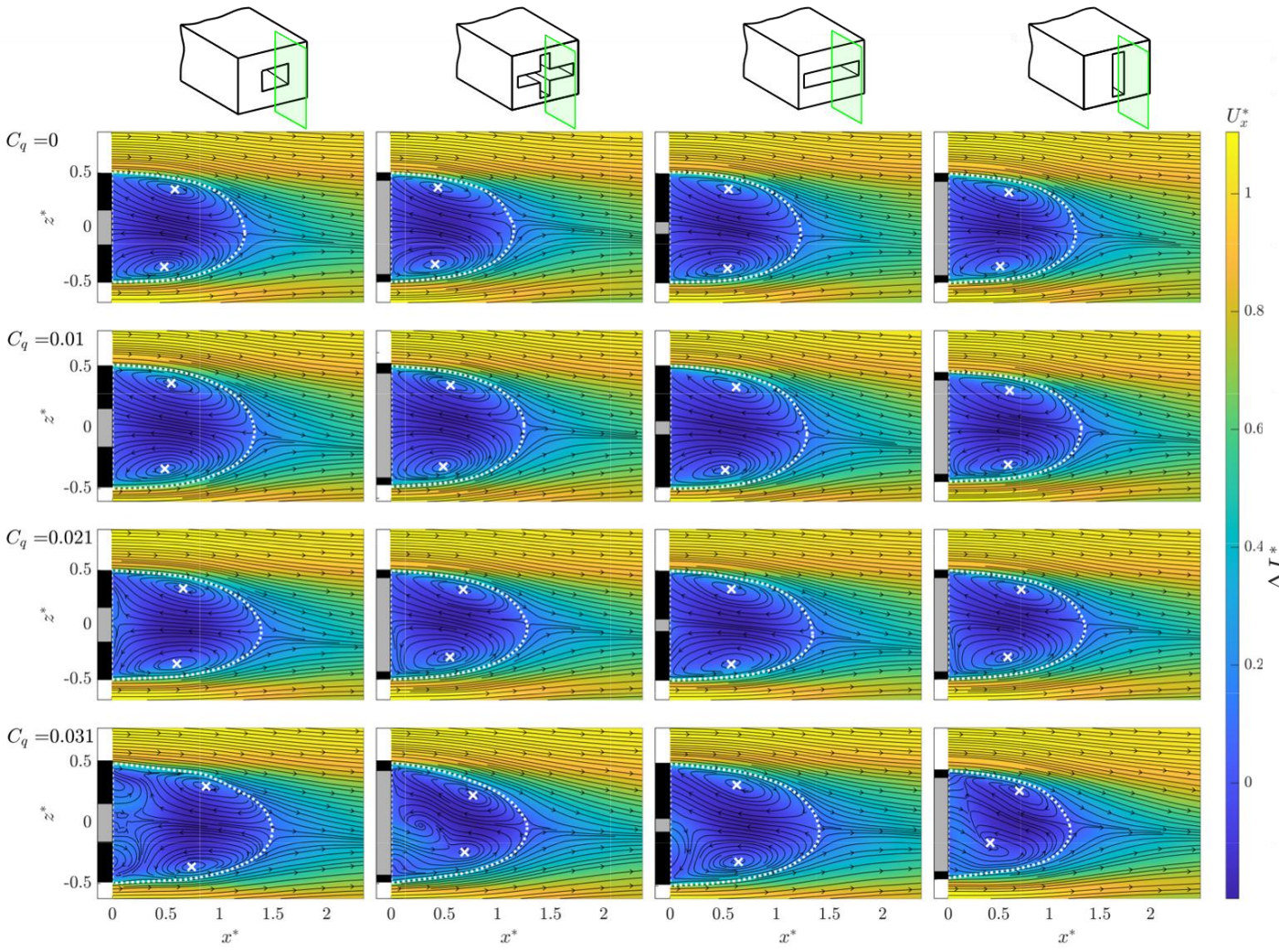

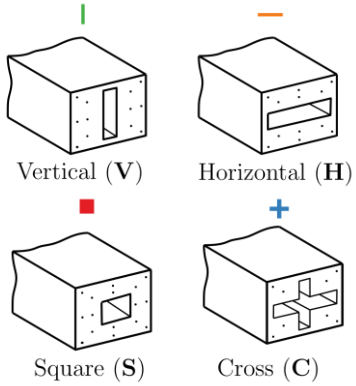

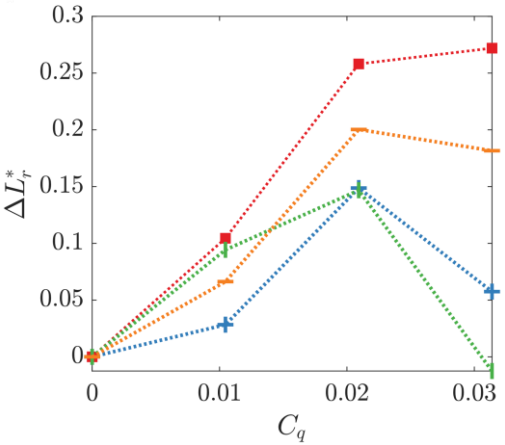

3. Results

- **Forces, pressure and recirculation bubble length**

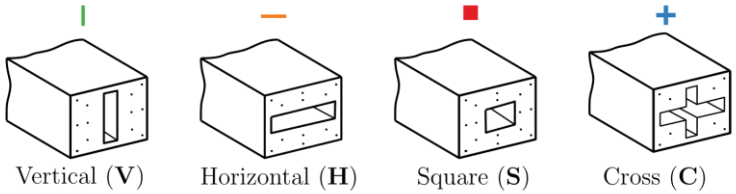

$$\left.\begin{aligned}\Delta C_B &= C_B^k - C_B^B \\ \Delta C_x &= C_x^k - C_x^B \\ \Delta L_r^* &= L_r^{*k} - L_r^{*B}\end{aligned}\right\} k = [S, C, H, V]$$

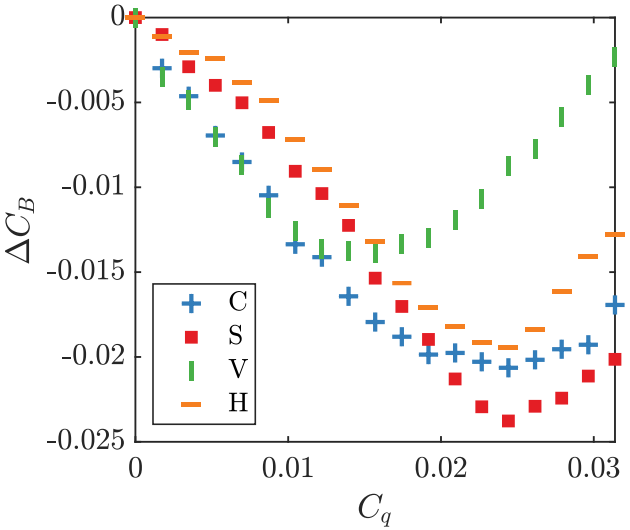

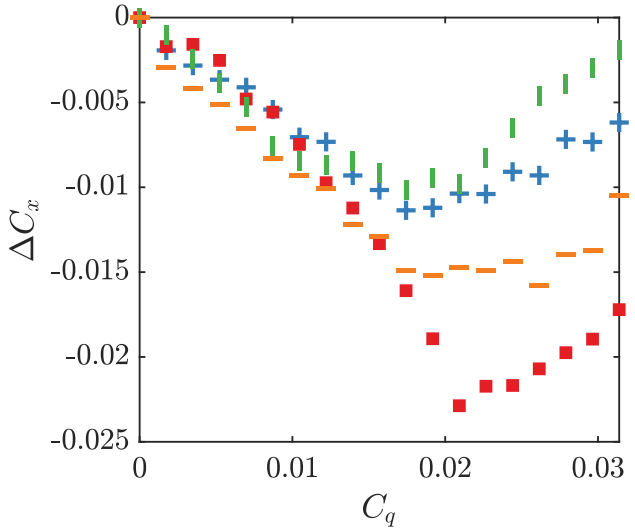

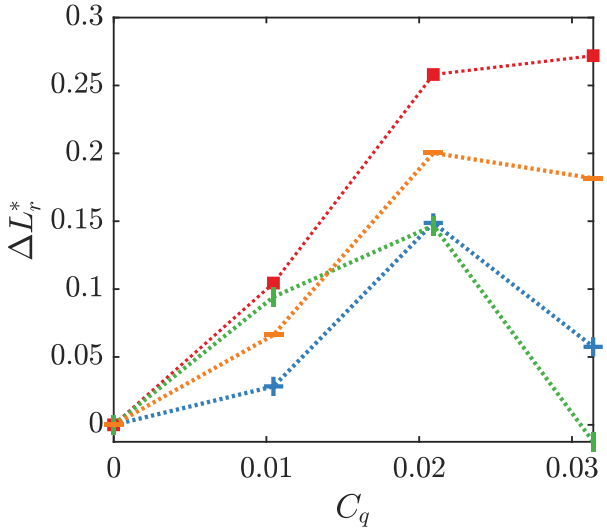

3. Results

➢ Forces, pressure and recirculation bubble length

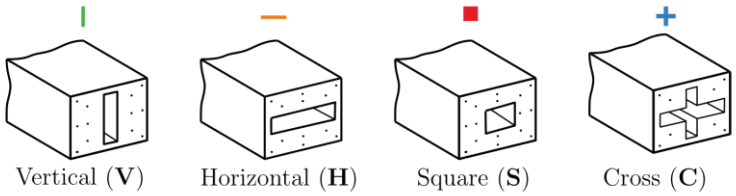

$$\left.\begin{aligned}\Delta C_B &= C_B^k - C_B^B \\ \Delta C_x &= C_x^k - C_x^B \\ \Delta L_r^* &= L_r^{*k} - L_r^{*B}\end{aligned}\right\} k = [S, C, H, V]$$

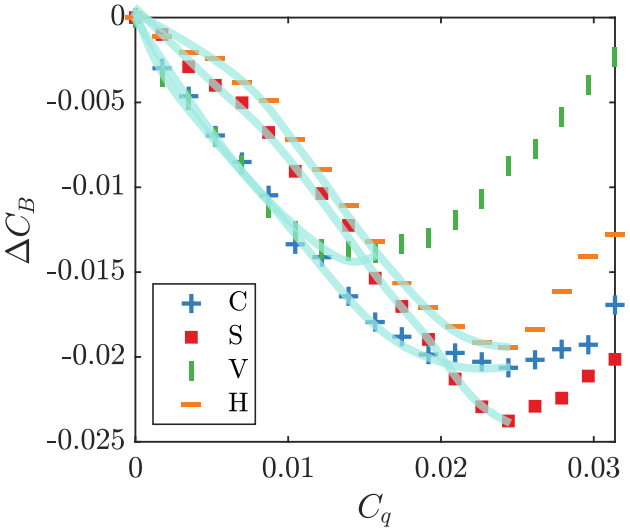

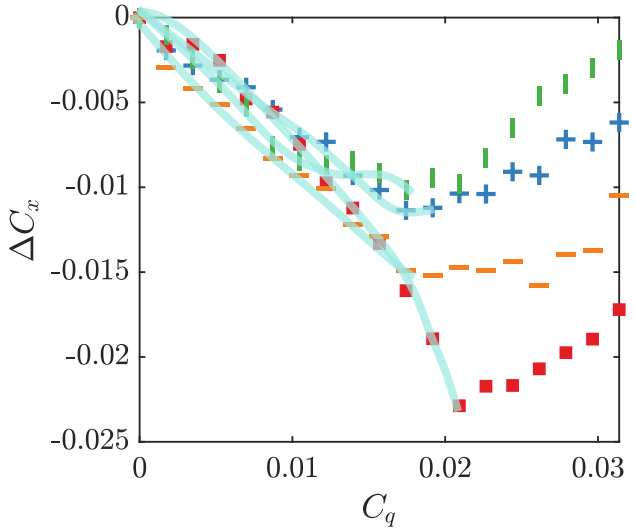

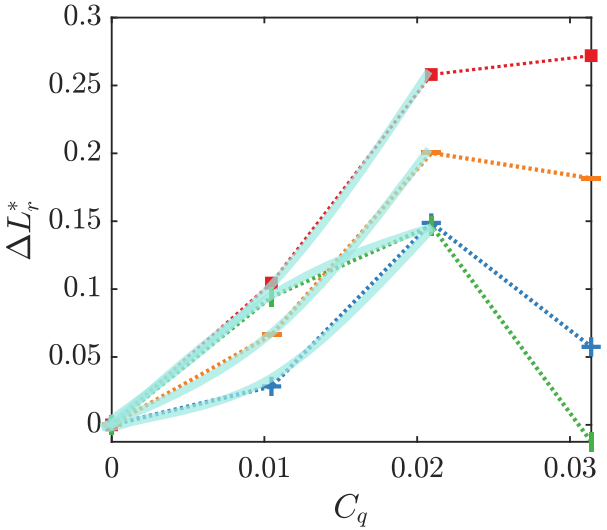

- Two regimes are identified in all slot configurations:
  - Mass regime: As C_q rises, the blowing jet fills recirculation bubble enhancing its length ($L_r^* \uparrow$) → Increasing base pressure ($C_B \downarrow$) → Reducing drag ($C_x \downarrow$)

3. Results

➢ Forces, pressure and recirculation bubble length

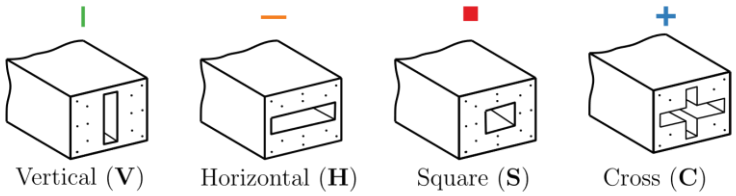

$$\left.\begin{aligned}\Delta C_B &= C_B^k - C_B^B \\ \Delta C_x &= C_x^k - C_x^B \\ \Delta L_r^* &= L_r^{*k} - L_r^{*B}\end{aligned}\right\} k = [S, C, H, V]$$

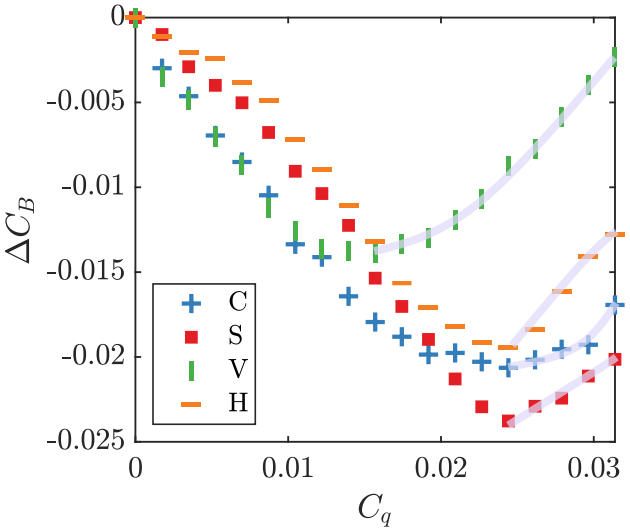

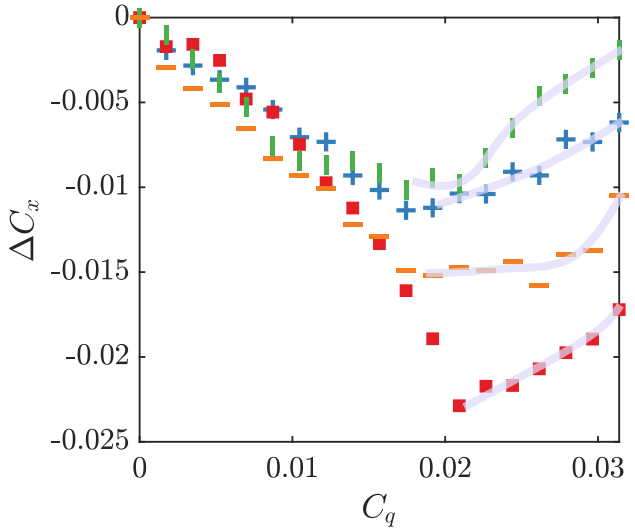

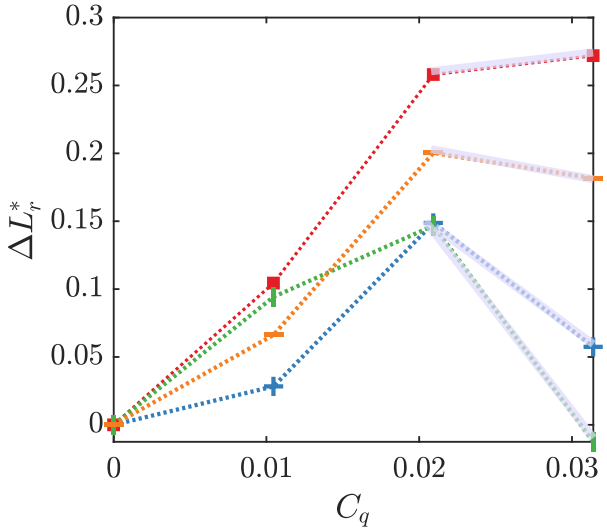

- Two regimes are identified in all slot configurations :
  - Mass regime: As C_q rises, the blowing jet fills recirculation bubble enhancing its length ($L_r^* \uparrow$) → Increasing base pressure ($C_B \downarrow$) → Reducing drag ($C_x \downarrow$)
  - Momentum regime: The jet starts to disturb the shear layers → The recirculation bubble shrinks ($L_r^* \downarrow$) → Reducing base pressure ($C_B \uparrow$) → Incresing drag ($C_x \uparrow$)

3. Results

➢ Forces, pressure and recirculation bubble length

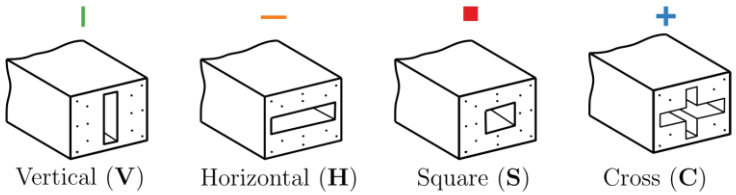

$$\left.\begin{aligned}\Delta C_B &= C_B^k - C_B^B \\ \Delta C_x &= C_x^k - C_x^B \\ \Delta L_r^* &= L_r^{*k} - L_r^{*B}\end{aligned}\right\} k = [S, C, H, V]$$

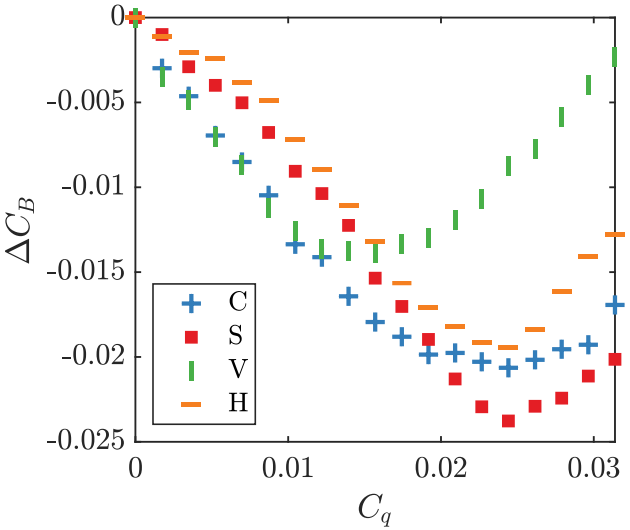

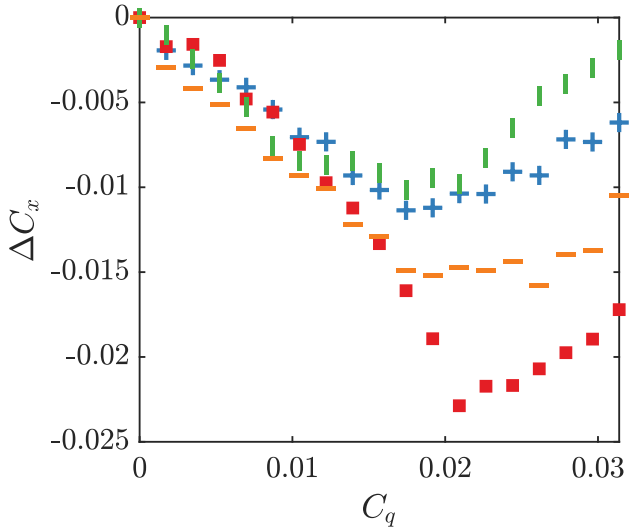

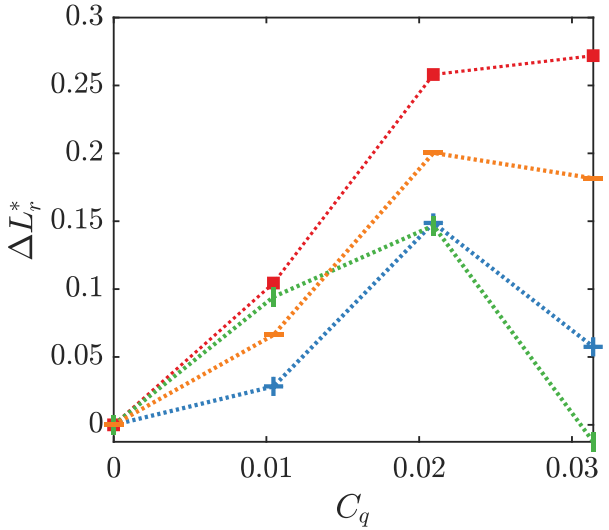

- Two regimes are identified in all slot configurations :
  - Mass regime: Curves tend to overlap
  - Momentum regime: Once the optimum value has been exceeded, the slots show clear differences.

3. Results

➢ Forces, pressure and recirculation bubble length

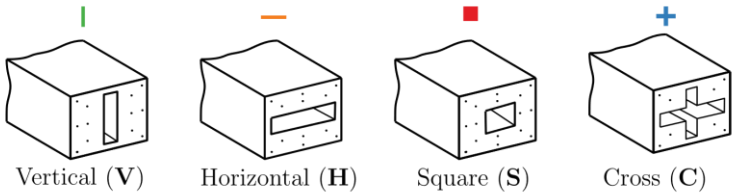

$$\left.\begin{aligned}\Delta C_B &= C_B^k - C_B^B \\ \Delta C_x &= C_x^k - C_x^B \\ \Delta L_r^* &= L_r^{*k} - L_r^{*B}\end{aligned}\right\} k = [S, C, H, V]$$

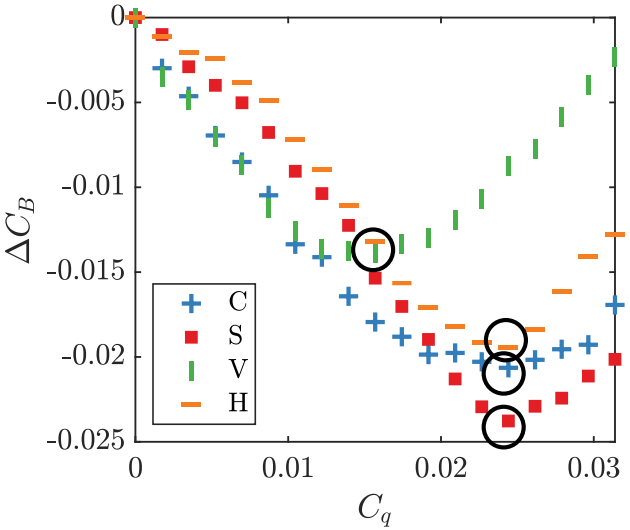

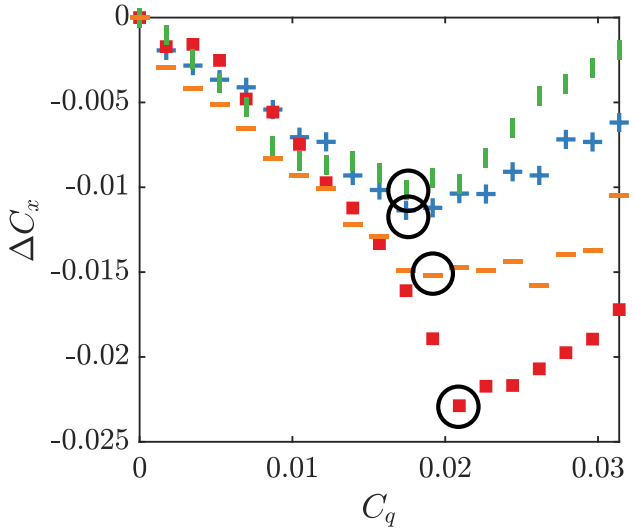

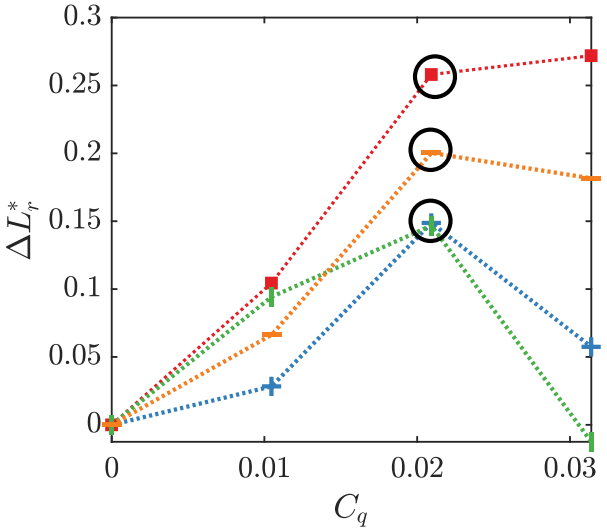

- Differences between the slots:
  - The **S** slot is the most efficient.
  - The vertical slots distribution (**V** and **C**) reduces drag very slightly.
  - **H** is an intermediate case between the above.

3. Results

➢ Reflexional symmetry breaking (RSB)

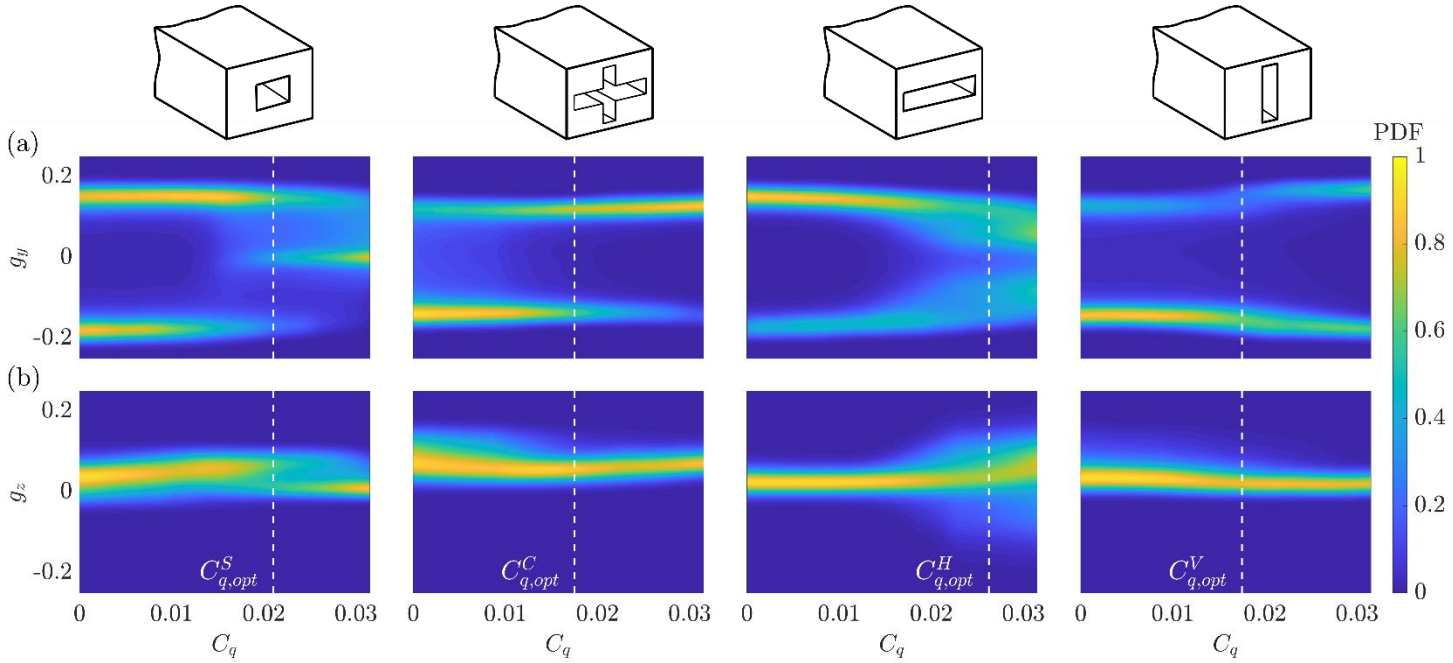

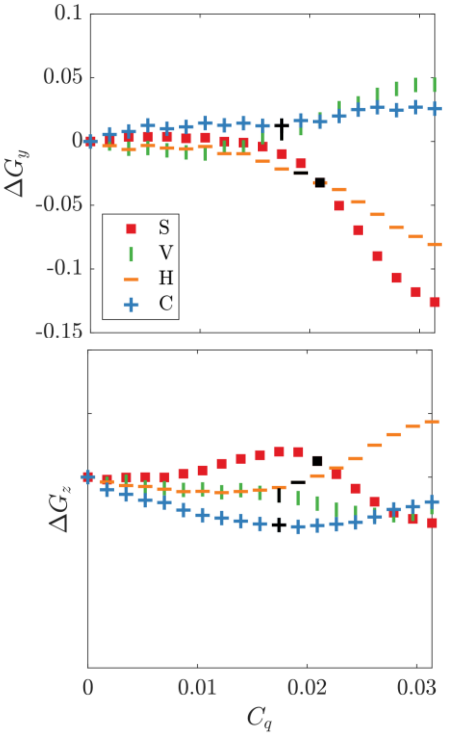

- RSB modes:
  - The vertical slots (**V** and **C**) asymmetrize the wake in the momentum regime.
  - The **S**-slot completely mitagate bi-stability and the **H**-slot tends to it.

4. Discussion

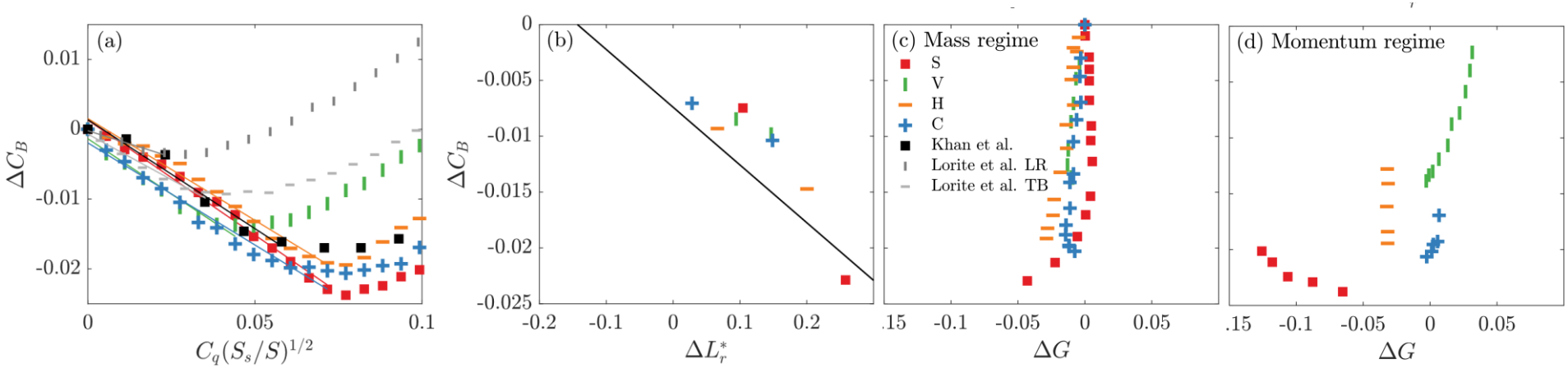

Slot	Geometry	S_s/hw	$C_{q,opt}$	$C_{q,opt}\sqrt{S_s/hw}$	$\Delta C_{B,max}$	Slope
S ■		0.1	0.0244	0.0772	-0.0238	-0.329
V ▮		0.1	0.0157	0.0496	-0.0139	-0.317
H ▬		0.1	0.0244	0.0772	-0.0194	-0.292
C ✚		0.1	0.0244	0.0772	-0.0206	-0.293
Khan et. al x1.0 ■		0.0057	0.0053	0.0708	-0.0170	-0.312
Khan et. al x0.5		0.001425	0.0027	0.0711	-0.0165	-0.315
Khan et. al x0.35		0.000698	0.0018	0.0672	-0.0166	-0.306
Lorite-Diez et al. LR ▮		0.0354	0.0055	0.0291	-0.0036	-0.152
Lorite-Diez et al. TB ▬		0.0498	0.0078	0.0347	-0.0093	-0.311

5. Conclusions

Two regimes (**mass** and **momentum**) have been identified in all configurations.

$C_q = 0$ **Mass regimen**

- The blowing jet fills recirculation bubble enhancing its length ($L_r^* \uparrow$) → base pressure recovery ($C_B \downarrow$) → drag reduction ($C_x \downarrow$).
- Here, $\Delta C_B = f(C_q\sqrt{S/S_s}) \approx -0.3\, C_q\sqrt{S/S_s}$ for all slot configurations, orientations or positions → ΔC_B and ΔC_x curves overlap.
- No major changes in RSB modes.

5. Conclusions

Two regimes (**mass** and **momentum**) have been identified in all configurations.

- The high-momentum jet starts to disturb the near wake topology and to produce an unstable jet → Drag reduction stops
- $\Delta C_{x,max}^S > \Delta C_{x,max}^H > \Delta C_{x,max}^C > \Delta C_{x,max}^V$
- **S** symmetries the wake (total suppression of bi-stability).
- **H** slightly symmetries the wake: partial suppression of bi-stability.
- The vertical slots (**V** and **C**) increase the horizontal wake asymmetry: less ΔC_B and $\Delta C_{x.}$

Thank you for your attention
Questions?

The authors gratefully **acknowledge** the funding provided by the projects TED2021-131805B-C21 and TED2021-131805B-C22, financed by the Spanish MCIN/ AEI/10.13039/501100011033/ and the European Union NextGenerationEU/PRTR.

Contact: jmcamach@ujaen.es